

**EXPERIMENTAL STUDY OF THERMAL/FORCE LOADS
ON SAMPLES IN A SUBSONIC CHANNEL**

V.A. Karpov, V.I. Lagutin, I.N. Murzinov, N.B.Plevako, and S.L. Zolotarev

Central Research Institute of Machine Building
141070 Korolev, Moscow Region, Russia

A Big Subsonic Channel as a part of the U-15T-2 set is intended to investigate the behavior of heat protection large-scale samples (~300 mm in length) in the environment of high-enthalpy gas flow at turbulent boundary layer conditions.

The test scheme is shown in Fig. 1. The sample has a shape of spherically blunted long cone with a cover made from a studied material. The sample is placed into a cone shroud connected with the heater. The sample is fixed on a rod with a strain-gauge balance, the rod is connected with a device of the sample movement.

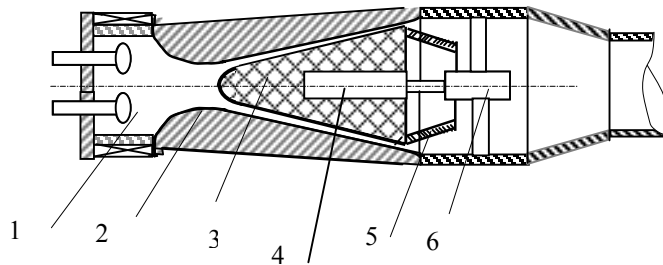


Fig.1. BSC test scheme.

1 –heater; 2 – channel; 3- tested sample; 4 – strain-gauge balance; 5 – back protection shell;
6 – sample moving device.

The channel design provides that the area of the gap between the model and the channel cones is closely the same along the surface and sonic flow is located at the model bottom. The model bottom diameter decreases due to ablation and, to keep the gap area, the model is automatically moved upstream, the movement is controlled by the heater pressure.

When heat protection cover is heated, recession rates of its binder and reinforcement (fabric as a rule) are different, so a relief develops on the surface, which can induce additional forces and moments due to interaction with the flow. The aerodynamic six-component strain-gauge balance mounted inside the model is intended for measurement of these forces and moments. The balance design particular features are considered in report [1], the main performance characteristics are given in the table below.

Characteristics	Components					
	X , kN	Y , kN	Z , kN	M_x , kN·cm	M_y , kN·cm	M_z , kN·cm
Nominal load	30	5	5	1	35	35
Resolution	0.05	0.008	0.008	0,0008	0.05	0.05
Main error , %	0,2%					

Typical plots of forces and moments measured by the balance are presented in Fig. 2.

Report Documentation Page

Report Date 23 Aug 2002	Report Type N/A	Dates Covered (from... to) -
Title and Subtitle Experimental Study of Thermal/Force Loads on Samples in a Subsonic Channel	Contract Number	
	Grant Number	
	Program Element Number	
Author(s)	Project Number	
	Task Number	
	Work Unit Number	
Performing Organization Name(s) and Address(es) Institute of Theoretical and Applied Mechanics Institutskaya 4/1 Novosibirsk 530090 Russia	Performing Organization Report Number	
	Sponsor/Monitor's Acronym(s)	
Sponsoring/Monitoring Agency Name(s) and Address(es) EOARD PSC 802 Box 14 FPO 09499-0014	Sponsor/Monitor's Report Number(s)	
	Distribution/Availability Statement Approved for public release, distribution unlimited	
Supplementary Notes See also ADM001433, Conference held International Conference on Methods of Aerophysical Research (11th) Held in Novosibirsk, Russia on 1-7 Jul 2002		
Abstract		
Subject Terms		
Report Classification unclassified	Classification of this page unclassified	
Classification of Abstract unclassified	Limitation of Abstract UU	
Number of Pages 5		

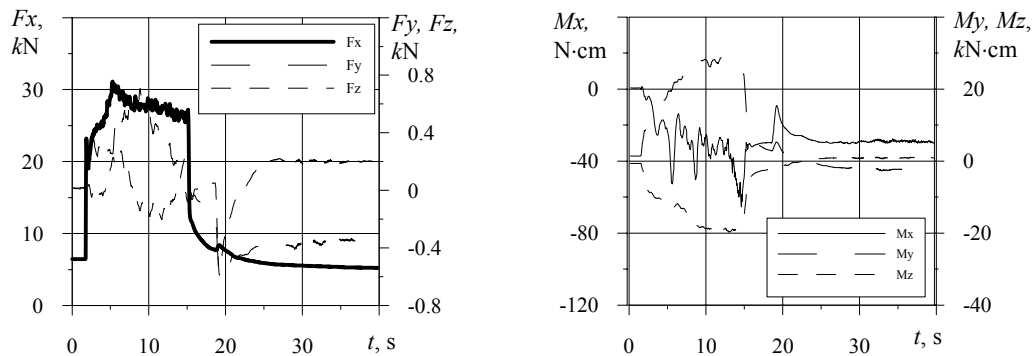


Fig. 2. Variation of forces and moments during a test.

Surface condition of tested sample is studied by means of roughness measurement both in longitudinal and transversal directions, measurement of shape with the use of coordinate-measuring machine UPCM (Opton Co, Carl Zeiss, Germany) and photo filming of the sample and its fragments.

Influence of surface roughness on, for example, rolling moment factor $m_x = Mx/SL(\rho V^2/2)$ is shown in Fig. 3. Values $(\rho V^2/2)$ correspond to the model bottom, S and L are the bottom area and length of the sample; roughness parameter Ra (average profile height [2]) is a medial one between that in longitudinal and in transversal directions. Though there is no obvious correlation between factor of moment m_x and parameter Ra , some tendency can be seen. Obviously, it is not roughness elements height itself that defines aerodynamic loads but orientation of the elements coupling with orientation of the model in the channel. If roughness elements orientation is random, it is only an average level of the induced loads that can be assessed.

The model shape measurement gives a possibility to find a variation along the sample generatrix of material loss thickness δ calculated as a distance between initial and final shapes. Figure 4 demonstrates a typical curve $\delta(s)$, where s – distance from the stagnation point along the surface. Fig.4 shows that heat flux distribution along the model generatrix is essentially non-uniform. In particular, the sharp increase in δ at $s \sim 55 \div 60$ mm indicates boundary layer transition.

Based on the after-test shapes analysis and corresponding transition criteria, algorithm for calculation of heat transfer in the subsonic channel had been developed. It was assumed that boundary layers of the sample and the channel develop independently till the point where the channel boundary layer achieves the sample surface or the sample boundary layer connects with the channel wall. Downstream this point the flow is considered as the gap flow and heat transfer is defined by mass overage parameters. The following correlations using the effective length method [3] were involved for laminar and turbulent heat transfer:

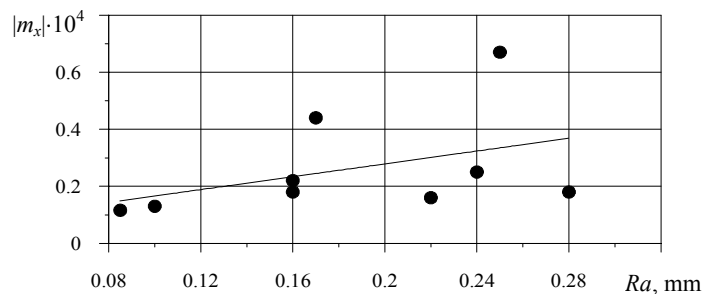


Fig. 3. Rolling moment factor dependence on roughness.

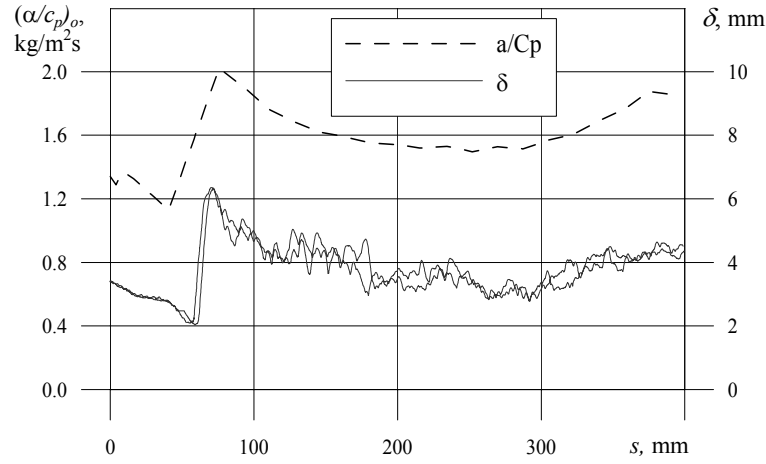


Fig. 4. Variation of material ablation thickness and heat transfer factor along a sample surface

$$q_{w,lam} = 0.332 \text{Pr}^{-2/3} \cdot \rho^* \cdot U_{\delta} \cdot \text{Re}_l^{*-0.5} \cdot (H_{e,lam} - H_w) \cdot K_l$$

$$q_{w,turb} = 0.013 \text{Pr}^{-3/4} \rho^* U_{\delta} \cdot \text{Re}_{\Delta}^{-1/4} (H_{e,turb} - H_w)$$

$$\text{where } \text{Re}_l^* = \frac{\rho^* U_{\delta} l}{\mu^*}, \text{Re}_{\Delta} = \frac{\rho_{\delta} U_{\delta} \Delta}{\mu_{\delta}}, l = \frac{\int_0^x R^2 \rho^* U_{\delta} \mu^* (H_e - H_w)^2 dx}{R^2 \rho^* U_{\delta} \mu^* (H_e - H_w)^2},$$

K_l –coefficient accounting for pressure gradient and temperature factor , Δ -energy loss thickness.

To find pressure distribution along a gap between sample and channel, area of the gap cross-section is calculated as a tore segment and pressure is calculated by iterations to fit a given mass flow rate. Pressure along the sphere bluntness is calculated as $P(x)=P_{00}(1-ax^2+bx^4)$, a and b factors are determined from the term of the function and its gradient continuity.

In response to the U-15T-2 jet non-uniformity, method of mass-average values ([4]) was involved. Enthalpy profile $H(R)$ is assumed as

$$\frac{H - H_n}{H_{axis} - H_n} = 1 - \left[1 - (1 - R)^{N/2} \right]^2,$$

where values H_n and N are determined from the term of mass and energy conservation laws. In accordance with the mass-average values method, a variable of flow function is introduced as

$$\psi = \frac{1}{2\pi} \int_0^R R \rho \cdot U \cdot dR$$

and dependence of total enthalpy on flow function is calculated both for the sample and the channel as

$$H_o = \frac{1}{\psi} \int_{\psi_o}^{\psi} H(\psi) d\psi.$$

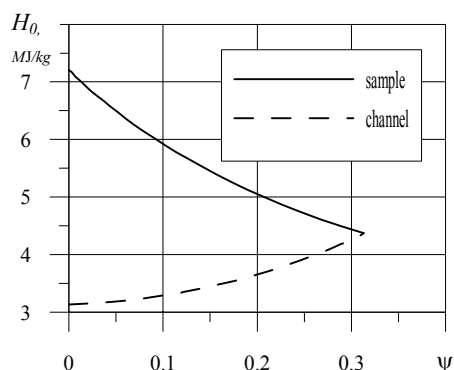


Fig. 5. Total enthalpy dependence on flow function

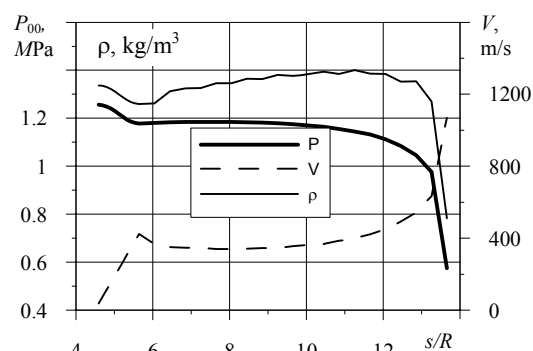


Fig. 6. Flow parameters variation along the sample surface

Typical dependence of total enthalpy on flow function for the sample and the channel is shown in Fig. 5. Calculations were conducted for the case of pressure in the heater $P_{00}=1.25\text{MPa}$, mass-average total enthalpy $H_{00}=4.6\text{ MJ/kg}$, mass flow rate $G=1.8\text{ kg/s}$. As an illustration of the calculation results, Fig. 6 shows variation of pressure P , flow velocity V and density ρ along the sample generatrix.

The calculated curve of heat transfer factor $(\alpha/c_p)_0$ for smooth impenetrable surface is shown at the plot Fig.4. Length of laminar zone is defined by a well-known correlation

$\bar{Re}_g = A \cdot e^{0.2M}$, where factor A is chosen equal to 165 to fit after-test shape. Extension of transition zone follows from correlation $Re_{g,end} = 1.5Re_{g,begin}$ [5]. It can be seen that the assumed mathematical model reflects in general the real heat transfer variation along the model generatrix.

Experimental data on measurement of heat flux and pressure variations along the sample cone surface are given in Figs. 7 and 8. Figure 7 shows variation with time of heat flux

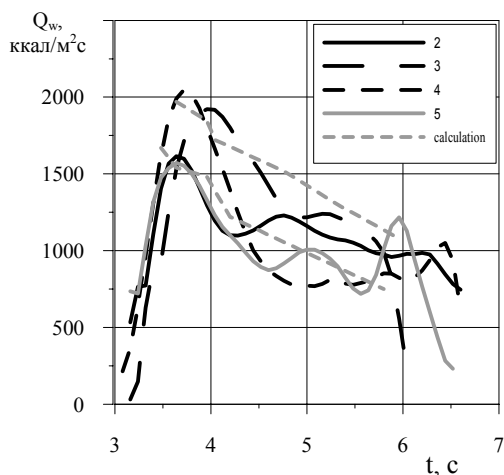


Fig. 7. Heat flux history measured and calculated in 4 points on cone surface

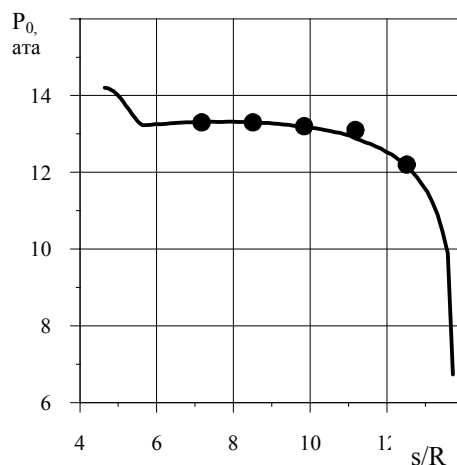


Fig. 8. Pressure variation along the cone surface, calculated and measured

measured in 4 points along the surface. Calculation results for the test conditions are presented as a band between two dotted lines on the same plot. The upper line corresponds to the point 5 (50 mm from the sample bottom), the lower one corresponds to the point 3 (the cone generatrix middle). Correlation of experimental and calculated data on pressure distribution is given in Fig. 8. It can be seen that there is a rather good coincidence of experimental and calculated data.

The presented experimental technique for Big Subsonic Channel supported by the flow parameters and heat transfer calculation software increases essentially possibilities of experimental investigation of heat protection material behavior in turbulent heat transfer condition and of ablation surface relief influence on force loads.

REFERENCES

1. **Lagutin V., Lapygin V.** Typical Balance Test Tasks for Aerogasdynamical Facilities of TSNIMash // Proc. of the First Intern. Symp. on Strain Gauge Balances, NASA/CP-1999-209101, NASA Langley Research Center, 1999. P. 385-392.
2. **Гжиров Р.И.** Краткий справочник конструктора. М.: Машиностроение, Ленингр. отд-ние, 1983. С. 123-128.
3. **Авдеевский В.С. и др.** Основы теплопередачи в авиационной и ракетно-космической технике. М.: Машиностроение, 1975.
4. **Сафиуллин Р.А.** Теплообмен в области прехода ламинарного пограничного слоя в турбулентный // Изв. АН СССР, МЖГ. 1971. № 6.
5. **Луцев В.В.** Метод среднemasовых величин для пограничного слоя во внешнем потоке с поперечной неоднородностью // Изв. АН СССР, МЖГ. 1967. № 1.